J|A|C|S COMMUNICATIONS

Published on Web 07/01/2010

Infrared-Active Heterostructured Nanocrystals with Ultralong Carrier Lifetimes

Doh C. Lee, István Robel, Jeffrey M. Pietryga, and Victor I. Klimov*

Center for Advanced Solar Photophysics, MS-J567, Los Alamos National Laboratory, Los Alamos, New Mexico 87545

Received March 31, 2010; E-mail: klimov@lanl.gov

Abstract: We present the synthesis of composite PbSe/CdSe/CdS nanocrystals with two distinct geometries: core/shell/shell structures and tetrapods. These novel nanostructures exhibit extremely long carrier decay times up to 20 μs that are combined with high emission efficiencies in the infrared. The increase in carrier lifetimes is attributed to the reduction of the electron−hole overlap as a result of delocalization of the electron wave function into the outer CdS shell or arms. The ultralong carrier lifetimes and controlled geometry render these nanocrystals attractive for a variety of applications from lasing to photocatalysis and photovoltaics.

A hallmark of colloidal synthesis of nanocrystals (NCs) is facile control over electronic and optical properties made possible by structural fine-tuning.[1] Initially, efforts focused on increasingly precise size control as a method for manipulating band gap, followed by "inorganic passivation" to increase emission quantum yield (QY).[2] As the range of applications-of-interest has become more sophisticated, interest has turned to heterostructured architectures as a means to control carrier *dynamics* and *exciton−exciton interactions*. This type of control can be accomplished in hetero-NCs featuring a charge-separated excited state in which the reduction of electron−hole wave function overlap may result in an increased radiative lifetime.[3] Such systems can also be used to achieve a "single-exciton" optical-gain regime due to unusually strong exciton−exciton repulsion, which shifts the "absorbing" optical transition away from the emission line.[4] Finally, spatial separation of electrons and holes can facilitate charge extraction and transport in photovoltaics and photocatalysis. While a number of examples of such hetero-NCs are known,[3,5,6] very few with activity in the infrared (IR) energy region exhibit extremely low QYs, indicating that carrier lifetimes are defined by fast nonradiative processes thus negating the advantage of slow radiative recombination. Here, we report hetero-NCs with extremely long-lived and efficient IR photoluminescence (PL). We also demonstrate facile shape control between spherical core/shell/shell NCs and well-defined tetrapods which can be used to tailor the properties of these novel materials to the specific needs of a range of applications.

With an effective band gap tunable over an extensive IR range (from near its bulk band gap of 0.27 eV to greater than 1.5 eV) and highly efficient PL, PbSe NCs are an obvious selection as a starting point for creating the sought-after heterostructures. Moreover, PbSe/CdSe core/shell NCs, created by partial ion exchange of larger PbSe NCs,[7] are stable enough for further material adgrowth and exhibit surface sensitivity that implies that excited electrons are partially delocalized into the CdSe shell,[7] while the large valence band offset between PbSe[8] and CdSe[3] effectively confines excited holes to the PbSe core. Thus, here, we focus on creating larger heterostructured NCs that potentially allow even further electron delocalization outside the core region. Building on similar effects

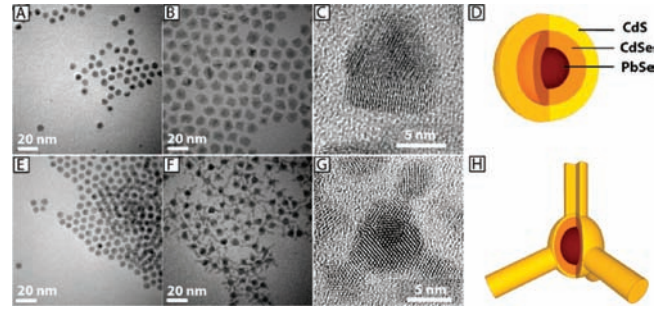

Figure 1. TEM images of PbSe/CdSe/CdS NCs prepared by CdS deposition. Injection of Cd and S precursors at 240 °C (A−D) or 170 °C (E−H) results in the final heterostructures with core/shell/shell or tetrapod geometries, respectively.

in CdSe/CdS core/shell NCs,[9] we targeted PbSe/CdSe/CdS core/shell/shell NCs.

PbSe/CdSe core/shell NCs used in our studies included a PbSe core of radius 19 Å with a 16 Å CdSe shell and an initial PL wavelength of 1340 nm. A CdS shell was grown by sequential addition of small amounts of cadmium oleate and elemental sulfur dissolved in 1-octadecene to the PbSe/CdSe NCs while stirring at 240 °C under inert conditions. (See Supporting Information.)

Changes observed in transmission electron microscope (TEM) images (Figure 1A−D) and PL spectra (Figure 2A) acquired from aliquots taken during precursor addition indicate two distinct stages of reaction. During the first stage, when the growth of the CdS shell is still negligible, PL QY rapidly diminishes and the PL band blue-shifts to ∼1240 nm. However, as the CdS shell growth proceeds, QY stabilizes (at ∼10%) and the emission peak moves back to the red approaching that of the original PbSe/CdSe seed NCs. A control study performed at 240 °C without CdS precursors confirms that the behavior during the initial phase is a result of heating, which causes annealing at the PbSe−CdSe interface without any measurable changes in the overall Pb:Cd ratio according to energy dispersive X-ray spectroscopy. This annealing, however, results in the reduction of the effective size of the pure PbSe core as ion exchange between the core and the shell leads to formation of an intermediate higher-band gap ternary alloy layer. This confines a hole to an effectively smaller volume, which leads to a blue shift of the emission band. On the other hand, this process may increase electron delocalization into the shell by "smearing out" a potential barrier at the PbSe/CdSe interface. The resulting increased exposure of electrons to surface traps is likely responsible for the steady decline in the QY until the CdSe surface is better passivated by the nascent CdS shell.

The red shift observed with increasing CdS thickness in the second stage of the reaction is consistent with increased electron delocalization due to expansion of the electron wave function into the outer CdS shell (Figure 2B). This reduces the electron confinement energy and leads to the decrease of the effective band

10.1021/ja102716p

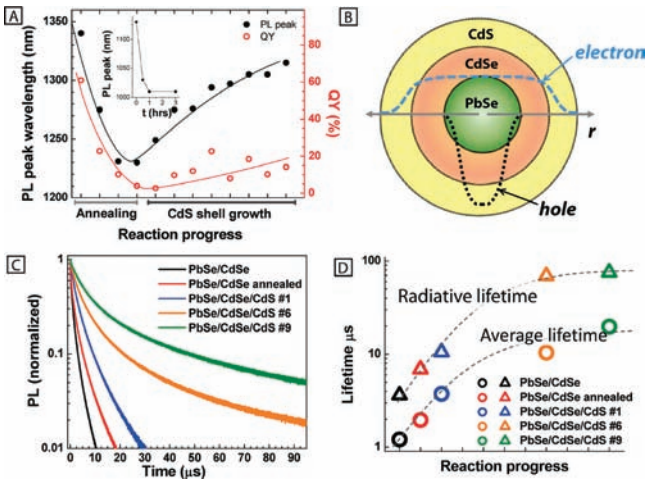

Figure 2. (A) PL peak position and QY of PbSe/CdSe/CdS core/shell/shell NCs at different stages of CdS shell growth at 240 °C. The first two data points correspond to aliquots taken at room temperature and at 240 °C before injecting Cd and S precursors. The inset shows the PL peak shift during controlled annealing (without CdS precursors) at 240 °C in 1-octadecene. QYs are not absolute but relative as measured against an IR dye, IR26, assuming the dye QY of 0.5%. (B) Illustration of possible electron and hole wave function distributions in a PbSe/CdSe/CdS NC. (C) Time-resolved PL decay of PbSe/CdSe/CdS NCs at different stages of the synthesis. (D) Average PL lifetimes and radiative time constants measured for different aliquots taken during CdS deposition.

gap. In fact, the effect of electron delocalization is likely even more significant than appears from the apparent PL red shift as it overcomes the competing increase in the confinement of the hole wave function due to annealing, which as the control study shows, continues throughout the reaction time.

The TEM analysis indicates that the CdS shell reaches the final thickness of up to 17 Å (Figure 1A−C). Although the initial PbSe/CdSe seed NCs are highly spherical, the final core/shell/shell particles appear to be irregularly shaped; however, the overall size distribution is only moderately increased.

Additional evidence of increased electron delocalization in PbSe/CdSe/CdS NCs, and concomitant reduction in the electron−hole wave function overlap, is provided by time-resolved PL studies (∼1 ns time resolution; see Supporting Information). We observe a moderate increase in the average PL lifetime (from ∼1 to ∼2 μs) during the annealing stage (Figure 2C and D). However, as the CdS shell grows thicker, the PL decay becomes multiexponential and the average time constant increases by an order of magnitude up to 20 μs. The modest QYs imply that PL decay is still dominated by nonradiative processes. If we analyze the longest PL component, which is typically attributed to radiative decay, we obtain a time constant of >80 μs! This is nearly 2 orders of magnitude longer than the ∼1 μs PL lifetime in PbSe NCs with the same PL wavelength (∼1240 nm); PbSe NCs of the same volume as our hetero-NCs (and therefore longer wavelength) would show even faster PL dynamics. The observation of ultralong exciton lifetimes is consistent with the schematic in Figure 2B, according to which the hole is confined to the PbSe core while the electron is delocalized over the entire volume of the core/shell/shell NC. Such spatial distribution of carriers produces a reduced electron−hole overlap and consequently slows electron−hole recombination.

To limit the deleterious effects of annealing on PL QY, CdS shell growth was also attempted at a lower temperature. In contrast to reactions at 240 °C, CdS growth performed at 170 °C showed only a very small blue shift before red-shifting to energies even lower than those in the original PbSe/CdSe NCs (Figure 3A).

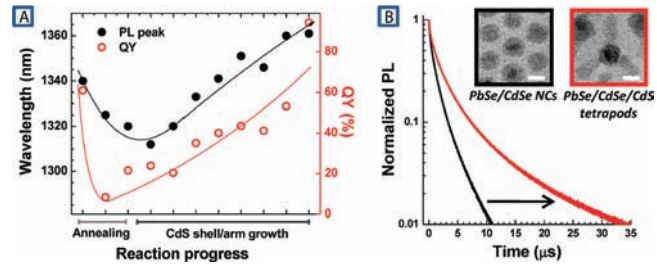

Figure 3. (A) PL peak wavelength and QY of PbSe/CdSe/CdS samples grown at 170 °C. (B) Time-resolved PL decay of PbSe/CdSe NCs (black) and PbSe/CdSe/CdS tetrapods (red). Inset: scale bars are 5 nm.

Moreover, CdS growth was accompanied by essentially complete recovery of QY. Surprisingly, TEM revealed that these particles did not grow as core/shell/shell, but as tetrapods with CdS arms (Figure 1E−H). The core of the heterostructures increased from 6.7 nm to ∼7.2 nm on average and became slightly more faceted, taking on a roughly tetrahedral appearance in many cases. The arms varied in size, reaching up to 7−9 nm in length, while their width remained fairly consistent at 2.5 nm. Although the crystal structure of the PbSe/CdSe core is cubic,[7] high-resolution TEM shows that the CdS arms are hexagonal wurtzite, with growth occurring in the (001) direction (see Supporting Information). Addition of a precursor at lower temperatures may have delayed the onset of growth and caused a higher degree of supersaturation and a subsequent fast-growth "surge," resulting in one-dimensional crystal growth akin to that observed in CdSe/CdTe tetrapods.[10]

The PL decay traces (Figure 3B) reveal that, as in core/shell/shell hetero-NCs, the red shift in tetrapods is accompanied by an increase in the PL lifetime, implying that electron density is again drawn away from the core. However, the effect is more moderate, with the average lifetime up to 2.4 μs, and with much higher PL QYs which can even exceed that of the original PbSe/CdSe NCs. This represents a significant departure from previously demonstrated hetero-NC systems in which an increase in radiative lifetime is always accompanied by introduction of significant nonradiative losses that lead to a dramatic reduction of emission efficiencies.[3,11]

In combining efficient emission in the IR with exceptionally long exciton lifetimes and controlled geometry (core/shell/shell NCs vs tetrapods), these novel hetero-NCs are of great potential utility. This type of simple but flexible control of recombination dynamics through chemical means may enable a class of materials in which carrier separation is tunable to the demands of the application. For example, for NC lasing, a significant reduction in the electron−hole overlap is key to achieving "single-exciton" optical gain, meaning that a core/shell/shell motif, which provides a greater extension of radiative lifetime, is more appropriate. On the other hand, in applications requiring carrier extraction, either to generate photocurrent or to perform chemistry, introducing directional carrier separation will be as important as an absolute increase in lifetimes. In this case, the tetrapod geometry may become preferential as tetrapod arms can be readily contacted to a charge-collecting network or catalyst sites.

Acknowledgment. This material is based upon work within the Center for Advanced Solar Photophysics, an Energy Frontier Research Center funded by the U.S. Department of Energy (DOE), Office of Science, Office of Basic Energy Sciences (BES). J.M.P. acknowledges support by the Chemical Sciences, Biosciences and Geosciences Division of BES, U.S. DOE.

Supporting Information Available: Experimental details and definitions of recombination lifetime. This material is available free of charge via the Internet at http://pubs.acs.org.

References

(1) Murray, C. B.; Norris, D. J.; Bawendi, M. G. *J. Am. Chem. Soc.* **1993**, *115*, 8706–8715.
(2) Hines, M. A.; Guyot-Sionnest, P. *J. Phys. Chem.* **1996**, *100*, 468–471.
(3) Kim, S.; Fisher, B.; Eisler, H.-J.; Bawendi, M. G. *J. Am. Chem. Soc.* **2003**, *125*, 11466–11467.
(4) Klimov, V. I.; Ivanov, S. A.; Nanda, J.; Achermann, M.; Bezel, I.; McGuire, J. A.; Piryatinski, A. *Nature* **2007**, *447*, 441–446.
(5) Xie, R.; Zhong, X.; Basche, T. *Adv. Mater.* **2005**, *17*, 2741–2745.
(6) Zhong, H.; Scholes, G. D. *J. Am. Chem. Soc.* **2009**, *131*, 9170–9171.
(7) Pietryga, J. M.; Werder, D. J.; Williams, D. J.; Casson, J. L.; Schaller, R. D.; Klimov, V. I.; Hollingsworth, J. A. *J. Am. Chem. Soc.* **2008**, *130*, 4879–4885.
(8) Cui, D.; Xu, J.; Zhu, T.; Paradee, G.; Ashok, S.; Gerhold, M. *Appl. Phys. Lett.* **2006**, *88*, 183111.
(9) Garcia-Santamaria, F.; Chen, Y.; Vela, J.; Schaller, R. D.; Hollingsworth, J. A.; Klimov, V. I. *Nano Lett.* **2009**, *9*, 3482–3488.
(10) Manna, L.; Milliron, D. J.; Meisel, A.; Scher, E. C.; Alivisatos, A. P. *Nat. Mater.* **2003**, *2*, 382–385.
(11) Shieh, F.; Saunders, A. E.; Korgel, B. A. *J. Phys. Chem. B* **2005**, *109*, 8538–8542.

JA102716P